RSC Advances

PAPER

View Article Online
View Journal | View Issue

Cite this: *RSC Adv.*, 2020, **10**, 25370

Supramolecular interaction of sanguinarine dye with sulfobutylether-β-cyclodextrin: modulation of the photophysical properties and antibacterial activity†

Vidya Kadam,‡[a] Aarti S. Kakatkar,[b] Nilotpal Barooah,[a] Suchandra Chatterjee,[bc] Achikanath C. Bhasikuttan *[ac] and Jyotirmayee Mohanty *[ac]

Received 28th April 2020
Accepted 22nd June 2020

DOI: 10.1039/d0ra03823g

rsc.li/rsc-advances

The noncovalent host–guest interaction of sanguinarine (SGR), a benzophenanthridine alkaloid, with a nontoxic, water soluble sulfobutylether-β-cyclodextrin ($SBE_7\beta CD$, commercially available as Captisol) macrocyclic host has been investigated using ground-state optical absorption, and steady-state and time-resolved fluorescence measurements. The pH-dependent changes in the absorbance of the dye at 327 nm showed a pK_a value of 7.5, which has been shifted to 8.1 in the presence of $SBE_7\beta CD$. The changes in the pK_a values, absorption and fluorescence spectra, and fluorescence lifetime values of these two forms of SG with $SBE_7\beta CD$ indicate complex formation between them. The cationic form shows 3 times higher interaction towards $SEB_7\beta CD$ ($K = 1.2 \times 10^4$ M^{-1}) as compared to the neutral form ($K = 3.9 \times 10^3$ M^{-1}) which leads to a moderate upward pK_a shift (pK_a values of SGR shifted by more than 0.6 units). The subsequent fluorescence "turn off" was demonstrated to be responsive to chemical stimuli, such as metal ions (Ca^{2+} ions). Upon addition of Ca^{2+} ions, nearly quantitative dissociation of the complex was established to regenerate the free dye and result in fluorescence "turn on". Apart from improving the stability under ambient light conditions, the upward pK_a shift of SGR in the presence of $SBE_7\beta CD$ results in increasing the antibacterial activity of the $SBE_7\beta CD$:SGR complex compared to that of the free dye towards four pathogenic micro-organisms at the physiological pH range. This work further compares SGR interaction with parent β-cyclodextrin.

Introduction

Modulation of the photophysical properties achieved through noncovalent host–guest interaction has triggered a lot of research interest among scientists owing to their potential applications in sensors,[1] aqueous dye lasers,[2] organic electronics,[3] optical switches,[4] drug delivery,[5] *etc.* Of late it has been observed that the antibacterial activity/shelf-life of drug molecules increases substantially in the presence of macrocyclic hosts either by increasing the photo- and thermal stability or by modulating the pK_a of drug molecules.[6,7] The increase in the antibacterial activity leads to a reduction in the minimum inhibitory concentration (MIC), which is very promising for practical use.

Sanguinarine (SGR) is a benzophenanthridine alkaloid that exhibits several biological effects, especially antimicrobial, anti-inflammatory and anti-cancer properties.[8] It has been used in dental hygiene products and feed additives.[7] SGR has also been found to inhibit the growth of human cervical cancer cells through the induction of apoptosis.[9] A critical limitation of its medicinal application stems from its poor solubility (<0.3 mg ml^{-1} or 0.9 mM at 298.15 K).[10] Depending upon the pH of the solution, SGR exists in two different forms, iminium (SG^+, the therapeutically active form) and alkanolamine (SGOH, inactive form) in water with a pK_a value of ~7.5.[7,11] The poor solubility and the conversion of ~50% to the inactive SGOH form at physiological pH of 7.4, limit its use for biomedical applications, especially, for the antibacterial activity.[7] Different research groups have made efforts to enhance its antibacterial activity either by modifying its structure[12] or by introducing macrocyclic hosts[7] or addition of other antibiotics such as vancomycin/streptomycin along with EDTA to get cumulative enhancement.[13] In a recent study, we have shown the enhanced antibacterial activity of SGR towards a multi-drug resistant bacteria by introducing calixarene-capped silver nanoparticles.[14] The physicochemical properties including

[a]*Radiation & Photochemistry Division, Bhabha Atomic Research Centre, Mumbai 400 085, India. E-mail: bkac@barc.gov.in; jyotim@barc.gov.in; Fax: +91 22 2550 5151*

[b]*Food Technology Division, Bhabha Atomic Research Centre, Mumbai 400 085, India*

[c]*Homi Bhabha National Institute, Training School Complex, Anushaktinagar, Mumbai 400094, India*

† Electronic supplementary information (ESI) available: Additional figures and tables. See DOI: 10.1039/d0ra03823g

‡ Student of D. B. F Dayanand College of Arts and Science, Solapur, India.

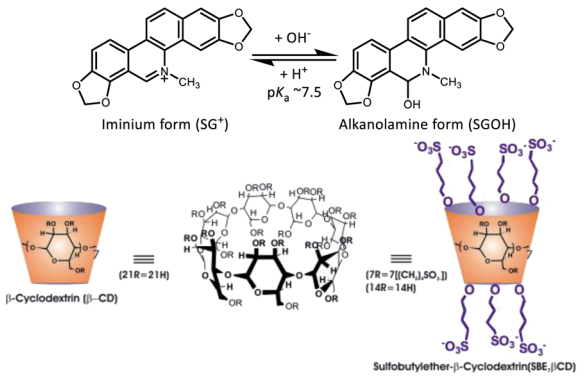

Chart 1 Chemical structures of the prototropic forms of SGR (SG^+ and SGOH) and the macrocyclic hosts, sulfobutylether-β-cyclodextrin ($SBE_7\beta CD$) sodium salt and β-cyclodextrin (βCD).

thermodynamic parameters of SGR with α-, β-, and γ-cyclodextrins have been reported by Hazra and co-worker.[10] Whereas, Biczok *et al.* have established the stabilization of SGR by cucurbit[7]uril (CB7) host by inhibiting the nucleophilic attack and photooxidation of SGR and effecting its release from CB7 cavity by controlling the pH of the solution.[15]

On the other hand, supramolecular host–guest interaction of water soluble sulfobutylether-β-cyclodextrin macrocycle (SBE_7-βCD; or Captisol) with organic guests (fluorescent dyes/drugs) has obtained enormous research interests in recent years owing to their several applications such as excipients in drug formulation,[16] for constructing stimuli-responsive on–off fluorescence sensor,[17] aqueous dye laser systems,[2] as amyloid fibril inhibitor[18] and supramolecular photosensitizer.[19] Having seven extended negatively charged sulfobutyl ether arms available at both the portals of βCD, the $SBE_7\beta CD$ is found to be very effective in modulating the molecular properties of cationic dyes/drugs through efficient host–guest interaction. In this work we have employed $SBE_7\beta CD$ macrocyclic host to modulate the photophysical properties as well as the antibacterial activity of SGR against two Gram negative: *Escherichia coli* (*E. coli*) and *Salmonella typhimurium* (*S. typhimurium*) and two Gram positive: *Bacillus cereus* (*B. cereus*) and *Staphylococcus aureus* (*S. aureus*) pathogenic bacteria. The results are also compared with the parent β-cyclodextrin host. The chemical structures of sanguinarine, $SBE_7\beta CD$ and βCD are provided in Chart 1.

Experimental

Materials

Sanguinarine chloride hydrate and sulfobutylether-β-cyclodextrin ($SBE_7\beta CD$) sodium salt with a degree of substitution of 6.4 were procured from Advent ChemBio Pvt. Ltd., India and used as received. The concentration of SGR solution was determined spectrophotometrically using its molar absorption coefficient ($\varepsilon = 30\ 700\ M^{-1}\ cm^{-1}$ at 327 nm in acidic aqueous solution).[15] Nanopure water (Millipore Gradient A10 System; conductivity of 0.06 μS cm^{-1}) was used to prepare the sample solutions. Luria Bertani broth, Luria agar, phosphate buffered saline were from HiMedia, Mumbai, India; 2,3,5 triphenyl tetrazolium chloride dye from Sigma chemicals.

Spectroscopic measurements

Optical absorption spectra and steady-state fluorescence spectra were recorded with a Shimadzu UV-Vis-NIR Spectrophotometer (UV-3600 plus, Tokyo, Japan) and FS5 spectrofluorometer (Edinburgh Instruments, UK), respectively. For steady state fluorescence measurements the samples containing SG^+ or SGOH forms were excited at isosbestic points (354 nm for SG^+) or at 340 nm for SGOH, where the changes in the absorbance were minimum in the absorption spectra. The time-resolved fluorescence measurements were carried out using a time-correlated single photon counting (TCSPC) set-up from Horiba Scientific (UK). In the present work, a 445 nm diode laser (100 ps, 1 MHz repetition rate) and 339 nm (<1 ns, 1 MHz repetition rate) were used for the excitation of SG^+ and SGOH forms, respectively. A reconvolution procedure was used to analyze the observed decays, which could be satisfactorily fitted by mono- or biexponential decay functions. The fluorescence decays [$I(t)$] were analyzed in general as a sum of exponentials,[20]

$$I(t) = \sum B_i \exp(-t/\tau_i) \quad (1)$$

where, B_i and τ_i are the pre-exponential factor and fluorescence lifetime for the i^{th} component, respectively. Reduced chi-square (χ^2) values (within 1.00–1.20) and random distribution of the weighted residuals among data channels were used to judge the acceptance of the fits.

For anisotropy measurements, samples were excited with a vertically polarized excitation beam, and the vertically and horizontally polarized fluorescence decays were collected with a large spectral bandwidth of ~32 nm. Using these polarized fluorescence decays, the anisotropy decay function, $r(t)$, was constructed as follows[20]

$$r(t) = \frac{I_V(t) - GI_H(t)}{I_V(t) + 2GI_H(t)} \quad (2)$$

$I_V(t)$ and $I_H(t)$ are the vertically and horizontally polarized decays, respectively, and G is the correction factor for the polarization bias of the detection setup. The G factor was determined independently by using a horizontally polarized excitation beam and measuring the two perpendicularly polarized fluorescence decays; measurements were repeated three times.

Isothermal titration calorimetric (ITC) measurements. ITC measurements were carried out using a Microcal iTC 200 from Malvern, UK. 200 μM of dye solution in the sample cell was titrated by adding consecutively 19 injections of 2 μl of 200 μM of $SBE_7\beta CD$ at pH 6.5 in phosphate buffer (10 mM) and at 25 °C. The first data point was removed from the data set prior to curve fitting with Origin 7.0 software. Thermodynamic parameters of the complex formation were also evaluated using the estimated binding constant value and molar reaction enthalpy (ΔH).

Antibacterial activity measurements. Antibacterial assay was carried out using 96-well Microtiter plates to determine the

minimum inhibitory concentration (MIC) which is defined as the lowest concentration of drug or antibacterial agent at which there is no visible growth of bacteria. The bacterial growth was confirmed visually by using 2,3,5 triphenyl tetrazolium dye. Standard bacterial cultures *B. cereus* (MTCC 430), *S. aureus* (MTCC 96), *E. coli* (ATCC 35218), *S. typhimurium* (MTCC 98) were used as the test bacteria.

The cells were inoculated from glycerol stock on Luria agar plate and loopful transferred to Luria Bertani broth and 50 μl was inoculated in fresh 5.0 ml broth incubated at 35 ± 2 °C on shaker 220 rpm for 18 h. These were then diluted to obtain a bacterial culture of 1×10^7 cfu ml^{-1} equal to turbidity of 0.5 McFarland's standard and used as working solution. 100 μl Luria broth was added to all the wells. 100 μl of sample was added to the first well and serially diluted two-fold from (80–2.5 μM) up to 6th well. 10 μl of either *E. coli* or *B. cereus* was added. 7th and 8th well served as positive and negative controls respectively. The plate was incubated for 18 h at 35 ± 2 °C with shaker at 220 rpm. 20 μl of tetrazolium dye was added to each well and further incubated for 20 minutes at 35 ± 2 °C. The change in colour of the dye indicates bacterial growth.

Results and discussion

Absorption spectral characteristics of sanguinarine with $SBE_7\beta CD$

SGR is a highly conjugated aromatic planar molecule. In aqueous solution, it exists in two different prototropic structures, namely cationic (SG^+) and neutral (SGOH) forms depending on the pH of the solution. At pH ~6.5, the protonated SG^+ form of the dye prevails and showed a characteristic absorption spectrum in the UV-Vis range of 280–600 nm (Fig. S1, ESI†) having a strong and sharp absorption peak at ~327 nm and a broad one around 470 nm.[10,14] The peaks at 327 and 470 nm correspond to the K and B absorption bands of the aromatic chromophore and the conjugated double bond, respectively, and arise due to the π–π* transitions of the molecule.[10,21] At higher pH ~9, the SGOH showed absorption peak at ~327 nm having no absorption band above 360 nm.[14] To account for this protolytic change and to estimate the pK_a of sanguinarine, the changes in the absorption spectra of the dye as a function of the pH of the solution are measured and are shown in Fig. S1, ESI.† The ground-state pK_a value estimated from the fitted curve of the data (*cf.* solid curve in the inset of Fig. S1, ESI†) was 7.5 ± 0.1 and is in good agreement with the reported values in the previous studies.[11,14]

In view of the pK_a value of 7.5 for the SGR dye, the interactions of two prototropic forms of SGR with $SBE_7\beta CD$ have been investigated at two pH values 6.5 and ~10.0. On gradual addition of $SBE_7\beta CD$ to the SG^+ in phosphate buffer solution at pH 6.5, the strong and narrow absorption band showed very small bathochromic shift (327 nm to 329 nm) along with hypochromic shift and got saturated with about 360 μM of $SBE_7\beta CD$ (Fig. 1A). Similarly as shown in Fig. 1B, upon addition of $SBE_7\beta CD$ to the SGOH solution at pH 10 (in bicarbonate buffer), only a very small (~2 nm) hypsochromic shift in the absorption peak was observed. These results show that prominent changes were

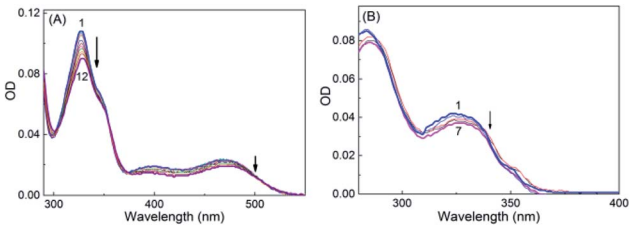

Fig. 1 (A) Absorption spectra of sanguinarine at different concentrations of $SBE_7\beta CD$ at pH 6.5. [$SBE_7\beta CD$]/μM: (1) 0.0, (2) 1.8, (3) 3.6, (4) 9.7, (5) 24.1, (6) 43.0, (7) 65.3, (8) 94.0, (9) 149.0, (10) 208.6, (11) 275.0 and (12) 360.0. (B) Absorption spectra of sanguinarine at different concentrations of $SBE_7\beta CD$ at pH 10. [$SBE_7\beta CD$]/μM: (1) 0, (2) 24, (3) 50, (4) 99, (5) 196, (6) 990 and (7) 1234.

observed in the absorption spectra of sanguinarine at pH 6.5 indicating significant interaction between $SBE_7\beta CD$ and SG^+. Whereas, only nominal changes in the absorption spectra at pH 10 shows weak interaction between $SBE_7\beta CD$ and SGOH. It may be noted here that both the forms of sanguinarine (pH 6.0 and 10.0) showed only negligible changes in their absorption spectra in the presence of the βCD host, indicating weak interactions between them (Fig. S2A and B,† ESI).

Fluorescence spectral characteristics of sanguinarine with $SBE_7\beta CD$

The fluorescence characteristics of these two prototropic forms of sanguinarine with $SBE_7\beta CD$ have been investigated. At pH 6.5, SG^+ displayed a broad emission spectrum (475–800 nm) with a peak at 607 nm.[14] Upon addition of $SBE_7\beta CD$ to the SGR in phosphate buffer at pH 6.5, the fluorescence spectra displayed red shift in the peak position (5 nm) along with considerable decrease in the emission intensity (Fig. 2A) and became saturated at ~360 μM of $SBE_7\beta CD$. At pH 10.0, SGOH in bicarbonate buffer solution displayed fluorescence spectrum in the wavelength range of 350 nm to 600 nm with a peak at 415 nm.[14] Strikingly, the emission band showed a significant increase in the fluorescence intensity along with a blue shift (~27 nm) in the peak position upon addition of $SBE_7\beta CD$ (Fig. 2B). From the plot of these intensity changes, the binding constant values estimated by using a modified Benesi–Hildebrand equation[22] (Method M1, ESI) are $(1.2 \pm 0.1) \times 10^4$ M^{-1} for $SBE_7\beta CD$:SG^+, $(3.9 \pm 1.0) \times 10^3$ M^{-1} for $SBE_7\beta CD$:SGOH complex (Insets of Fig. 2). This result also specifies that SG^+ exhibits ~3-fold stronger interaction with $SBE_7\beta CD$ as compared to the interaction of SGOH with $SBE_7\beta CD$.

Correspondingly for the comparison, the fluorescence characteristics of these two prototropic forms of sanguinarine with βCD host have also been investigated. Fig. S3A and B,† ESI are the fluorescence spectra of SGR with varying concentration of βCD at pH 6.0 and 10.0, respectively. The binding constant values estimated by using the modified Benesi–Hildebrand equation are $(1.4 \pm 0.6) \times 10^3$ M^{-1} for the βCD:SG^+, $(1.0 \pm 0.3) \times 10^4$ M^{-1} for the βCD:SGOH complex. In contrast to the interaction of $SBE_7\beta CD$, this result indicates that SGOH shows 10 times higher interaction with βCD as compared to the interaction of SG^+ with βCD.

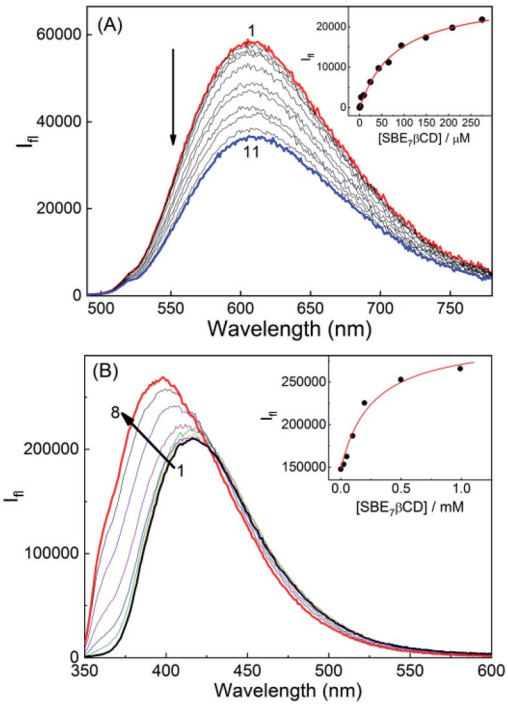

Fig. 2 (A) Fluorescence spectra of SG^+ at different concentrations of $SBE_7\beta CD$ at pH 6.5. [$SBE_7\beta CD$]/μM: (1) 0, (2) 1.8, (3) 3.6, (4) 9.7, (5) 24.1, (6) 43.0, (7) 65.3, (8) 94.0, (9) 149.0, (10) 208.6 and (11) 275.0. (B) Fluorescence spectra of SGOH at different concentrations of $SBE_7\beta CD$ at pH 10.0. [$SBE_7\beta CD$]/μM: (1) 0, (2) 24, (3) 50, (4) 99, (5) 196, (6) 498, (7) 990 and (8) 1234. Insets show the binding isotherms for the respective systems.

Isothermal titration calorimetric measurements

To further validate the proposed complex formation, isothermal titration calorimetric (ITC) measurements have been carried out to obtain the thermodynamic parameters. From the heat evolved during the titration the plot of integrated heat profile *versus* the mole ratio has been generated and are presented in Fig. 3. The ITC data obtained for $SBE_7\beta CD{:}SG^+$ and $SBE_7\beta CD{:}SGOH$ systems (Fig. 3) show good fittings with one-set-of-sites model indicating a 1 : 1 complex formationwith binding constant values of $(1.3 \pm 0.1) \times 10^4\ M^{-1}$ and $(0.9 \pm 0.3) \times 10^3\ M^{-1}$, respectively, which match well with the binding constant values obtained from the fluorescence titration data. The change in free energy values evaluated from enthalpy and, entropy values for these complexation processes for both SG^+ and SGOH forms with $SBE_7\beta CD$ are -5.6 kcal mol^{-1} and -4.4 kcal mol^{-1}, respectively and are energetically favourable.

Effect of $SBE_7\beta CD$ on the acidity constant (pK_a) of sanguinarine

Substantial changes in the protolytic equilibrium of the included guests are often come across in the host–guest interactions due to the preferential binding of one of the prototropic forms with the host.[23] The advantages of such pK_a shifts are vast and have been assessed for several applications.[24,25] Upward pK_a shifts are usually observed for weakly basic molecules in the presence of cation-

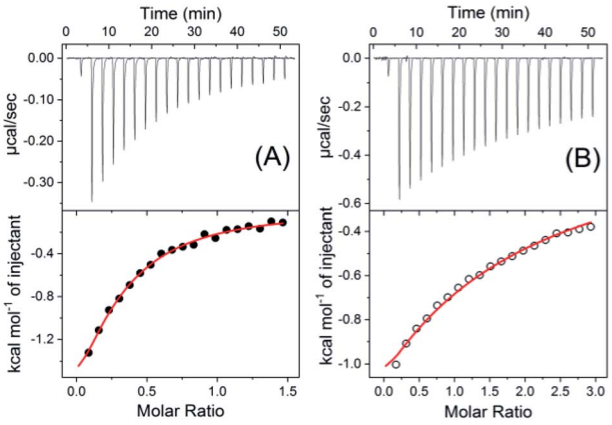

Fig. 3 Upper panels show the raw data for the titration of 200 μM SG^+ with 2 mM $SBE_7\beta CD$ at pH 6.5 in phosphate buffer (10 mM) (A) and 200 μM SGOH with 4 mM $SBE_7\beta CD$ at pH 9.0 (B) at 25 °C, showing the calorimetric response as successive injections of the host are added to the sample cell. Lower panels of (A) and (B) show the integrated heat profile of the calorimetric titrations. The solid line represents the best nonlinear least-squares fit to a sequential binding-site model.

receptor or hydrogen bond-acceptor hosts, while downward pK_a shifts are expected for anion-receptor, hydrogen bond donor host molecules or those offering a nonpolar cavity.[24] In this context, effect of $SBE_7\beta CD$ on the acid–base characteristics of sanguinarine was investigated by following the changes in the absorption spectra of the dye with varying pH, in the presence of 2 mM $SBE_7\beta CD$ (Fig. 4). In the present case, assuming the complexation of both the forms of the dye with $SBE_7\beta CD$, it appeared reasonable that the protolytic equilibria of the dye would follow a four-state model (Scheme 1).[23] K_a and K_a' represent the acid dissociation constants for the uncomplexed and complexed dye, respectively, and $K_{eq}{}^1$ and $K_{eq}{}^2$ represent the binding constants for the SG^+ and SGOH forms of the dye with $SBE_7\beta CD$. So, one can calculate the pK_a' value of the complex from the independently determined binding constants for the protonated and the neutral forms and the pK_a value of the unbound dye using eqn (3). A resulting pK_a' value of 8.0 thus calculated, suggests an adequate upward pK_a shift by 0.5 units.

$$K_a' = K_a K_{eq}{}^1(\mathrm{SGOH}) \Big/ K_{eq}{}^2(\mathrm{SG^+}) \qquad (3)$$

This upward pK_a shift calculated is further verified from the spectrophotometric pH titrations of sanguinarine both in the absence and presence of 2 mM $SBE_7\beta CD$, with changing the pH of the solution. A higher $SBE_7\beta CD$ concentration (2 mM) was employed to ensure virtually quantitative binding of both the prototropic forms of the drug with $SBE_7\beta CD$. The absorption spectral changes are significant at ~470 nm in the investigated pH range from 4–10 as shown in Fig. 4A and S1.† From this, the OD changes at ~470 nm *versus* pH has been plotted and the pK_a curves for the dye in the presence of $SBE_7\beta CD$ has been obtained (Fig. 4B and inset of Fig. S1, ESI†). The pK_a value obtained from the fitted curve is about 8.1 which matches well with the value obtained from the four-state model of Scheme 1. As discussed before in the light

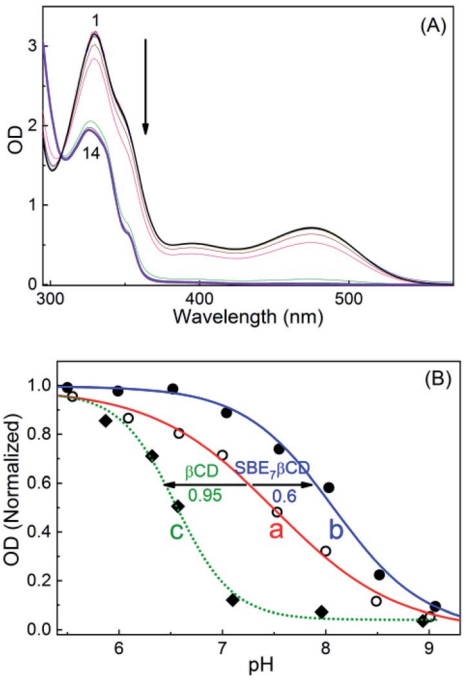

Fig. 4 (A) Absorption spectra of sanguinarine in the presence of 2 mM $SBE_7\beta CD$ at different pH values. pH: (1) 3.5, (2) 4.0, (3) 4.5, (4) 5.0, (5) 5.5, (6) 6.0, (7) 6.5, (8) 7.0, (9) 7.5, (10) 8.0, (11) 8.5, (12) 9.1, (13) 9.5, (14) 10.0. (B) pK_a curve of SGR in the absence (a) and presence of $SBE_7\beta CD$ (b) and βCD (c) (variation in absorbance with pH at 470 nm).

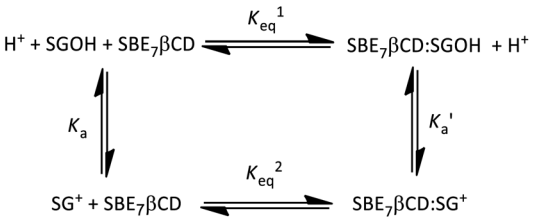

Scheme 1 Four-state thermodynamic model.

of binding constant values, the cationic form of the dye (SG^+) preferentially binds to $SBE_7\beta CD$ to form the inclusion complex, whereas its neutral form, SGOH, exhibits only a moderate interaction towards $SBE_7\beta CD$. Therefore, the reasonable increment in the pK_a values of SGR from ~7.5 to ~8.1 (Table S1, ESI†) in the presence of $SBE_7\beta CD$ is in line with the stabilization of the SG^+ by the $SBE_7\beta CD$ cavity as compared to the SGOH. On the other hand, the pK_a value of SGR decreases by ~0.95 unit (from 7.5 unit to 6.55, Fig. 4B, S4 and Table S1, ESI†) in the presence of 2 mM βCD host and matches well with the pK_a value of 6.65 obtained from four-state model corresponding to βCD host. This result indicates that SGOH form gets stabilized by the hydrophobic interaction imparts by the cavity of βCD.

Time-resolved fluorescence and anisotropy studies of sanguinarine in presence of $SBE_7\beta CD$

Fluorescence lifetime measurements of both the forms of SGR has been carried out to explore the effect of $SBE_7\beta CD$ and βCD

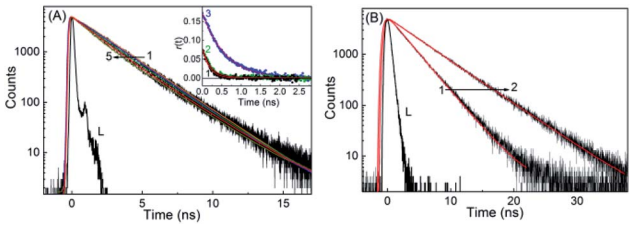

Fig. 5 (A) Lifetime decay traces of SG^+ form at different concentrations of $SBE_7\beta CD$ at pH 6.5. [$SBE_7\beta CD$]/μM: (1) 0, (2) 12, (3) 74, (4) 192 and (5) 350. λ_{ex} = 445 nm, λ_{em} = 605 nm. Inset: anisotropy decay traces of SG^+ in the absence (1) and presence of βCD (2) and $SBE_7\beta CD$ (3). (B) Lifetime decay traces of SGOH form in the absence (1) and presence (2) of 1.2 mM of $SBE_7\beta CD$ at pH 10. λ_{ex} = 339 nm, λ_{em} = 380 nm.

macrocyclic hosts on the excited states of the SGR at preset pH conditions. At pH 6.5, the decay trace of the protonated form of SGR recorded at 605 nm apparently shows a single exponential fitting with lifetime about 2.28 ns (Fig. 5). Upon gradual addition of $SBE_7\beta CD$ to the SG^+ solution, the decay trace becomes biexponential with the contribution of a short lifetime about ~0.84 ns (24%) along with the contribution from the free dye (Fig. 5A and Table S2, ESI†). Accordingly, the average lifetime of SG^+ decreases from ~2.28 ns to 2 ns in the presence of 350 μM concentration of $SBE_7\beta CD$. Whereas, only a slight decrease in the average lifetime (2.28 ns to 2.17 ns) is observed in the presence of 2.9 mM of β-CD host at pH 6.0 (Fig. S5 and Table S2, ESI†). Similarly, the changes in the excited state lifetime of SGOH is also probed at pH 10 in the absence and presence of $SBE_7\beta CD$ and βCD hosts. Unlike the SG^+ form, SGOH displayed relatively longer excited state lifetime of ~3 ns when probed at ~380 nm, corresponding to its emission maximum. Moreover, contrary to the decrease of the lifetime values as observed for SG^+, the SGOH in presence of $SBE_7\beta CD$ displayed an increase in the lifetime value to 5.11 ns (97%) with a contribution of 2.25 ns (3%) with the addition of 1.2 mM of $SBE_7\beta CD$ as shown in Fig. 5B (Table S2, ESI†). Further it is interesting to note that SGOH displayed a lifetime of ~5 ns in presence of 1 mM βCD as well (Fig. S5 and Table S2, ESI†), in accordance to the similarity in binding interactions, discussed before.

Further, the formation of the host–guest complex can also be confirmed from the change in the size of the fluorescing guest due to host–guest interaction. In this regard, fluorescence anisotropy measurements (see Experimental section for details) were carried out for SG^+ both in the absence and presence of $SBE_7\beta CD$ and βCD. As presented in the inset of Fig. 5A and Table S2, ESI,† the anisotropy decay time (τ_r) displayed 185 ps for SG^+ alone, 285 ps for the βCD:SG^+, whereas it displayed a significant increase to 575 ps in the $SBE_7\beta CD$:SG^+ system. This increase in the τ_r values due to the increase in the hydrodynamic volume of the emitting probe could be attributed to the complex formation with the βCD and $SBE_7\beta CD$ hosts.

Geometry optimization of the complex

To obtain more insight about the interaction and the ensuing geometry of both the prototropic forms (SG^+ and SGOH) of SGR

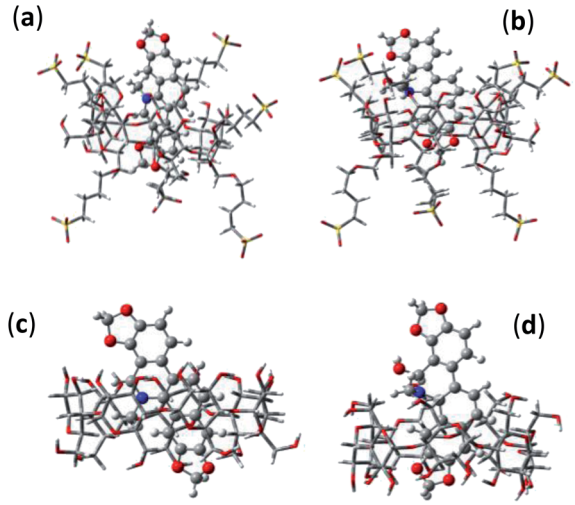

Fig. 6 Optimized geometries of 1 : 1 inclusion complexes of SBE_7-βCD:SG^+ (a), SBE_7βCD:SGOH (b), βCD:SG^+ (c) and βCD:SGOH (d).

with SBE_7βCD and βCD, computational calculations following semiempirical method were performed. The ground-state geometry of both the protonated and neutral forms of SGR and their 1 : 1 complexes with SBE_7βCD and βCD have been optimized at the PM3 level incorporating a molecular mechanics (MM) correction, using the Gaussian package.[26] In all the cases, geometry optimization was carried out without any symmetry constraint and in the absence of solvent. Care was taken to avoid any false minima, by using several input geometries, corresponding to the different anticipated conformations. The most stable structure was the one in which SG^+ is incorporated vertically along the center of the SBE_7βCD and βCD host cavities (Fig. 6) and the lowest ΔH_f values obtained for these arrangements are −186.1 kcal mol^{-1} and −9.5 kcal mol^{-1}, respectively. Higher $-\Delta H_f$ value obtained for SBE_7βCD:SG^+ complex as compared to βCD:SG^+ complex indicates the protonated form is better stabilized by the additional negatively charged sulfobutylether arms present in the SBE_7βCD. On the other hand, SGOH provided very nominal $-\Delta H_f$ value (ΔH_f = −5.3 kcal mol^{-1}) with SBE_7βCD where as with βCD the SGOH displayed energetics (ΔH_f = −9.1 kcal mol^{-1}) comparable to that of SG^+, where the interactions are mainly through hydrophobic and hydrogen bonding interactions. Note that the ΔH_f values corresponding to the complexes of both the protonated and neutral forms of SGR with SBE_7βCD and βCD correlates well with their binding constant values determined from the fluorescence titrations (Fig. 2).

Photostability of sanguinarine in the presence of SBE_7bCD

It has been recognised that the photostability of chromophoric dye and drugs increases substantially through inclusion complex formation with macrocyclic hosts,[6,27] where the dye/drug molecule gets stabilized/protected in their hydrophobic cavity. In this context, the photostability of SGR in the absence and presence of SBE_7βCD and βCD macrocyclic host has been investigated at ambient condition. The change in the absorbance at respective peak positions of the complexed and uncomplexed SGR at pH 7.4 was monitored at different time intervals with day light irradiation and the plots are presented in Fig. 7. It is seen that the photostability of SGR improved significantly in the presence of SBE_7βCD host as compared to the free SGR dye and βCD-complexed SGR. As demonstrated above the SG^+ interacts and forms an inclusion complex with SBE_7βCD stronger than the other host. In the inclusion complex, the guest dye is better rigidized and protected from other interactions which accelerates its degradation. Also, due to the upward pK_a shift of SGR in the presence of SBE_7βCD, the availability of SG^+ form increases and gets stabilized by SBE_7-βCD through cation–anion interaction.

Stimuli-responsive fluorescence off–on mechanism of SBE_7βCD:SGR assembly

After establishing that the assembly formation between SBE_7βCD and SGR switches off the fluorescence (605 nm), we attempted to disassemble the complex to switch on the fluorescence at pH 6.5. For this we have introduced another cationic additive such as Ca^{2+}, which can competitively interact with the negatively charged SBE_7βCD portals and replace the bound SGR. Gradual addition of Ca^{2+} ions to the SBE_7βCD:SG^+ complex successively increased the fluorescence emission. The changes in both the absorption and fluorescence spectra seen upon the initial titration were reversed (Fig. 8), thus demonstrating the rupture of the complex and the regeneration of the spectral features of free SG^+. Practically, the SGR fluorescence is turned off by ~50% on increasing the amount of SBE_7βCD, and the addition of Ca^{2+} ions (~100 mM) was able to achieve nearly complete breakage of the complex and switch on the fluorescence.

Antibacterial activity of SBE_7βCD:SGR assembly

As discussed in the introduction section, the iminium ion (SG^+) form of sanguinarine is responsible for the antibacterial activity. However, as the pK_a of the SG^+-SGOH falls around the region of the physiological pH (7.4) and both the forms are equally feasible at this pH, the efficacy of SGR's antibacterial activity at physiological pH is quite underestimated.[5,13] In this context, we explore the feasibility of using the above

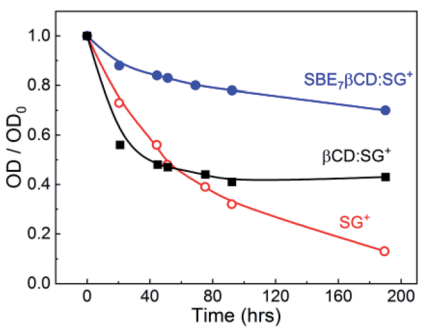

Fig. 7 The changes in absorbance at the peak positions with time of SGR in the absence and presence of SBE_7βCD (2 mM) and βCD (2 mM), at ambient conditions at pH 7.4.

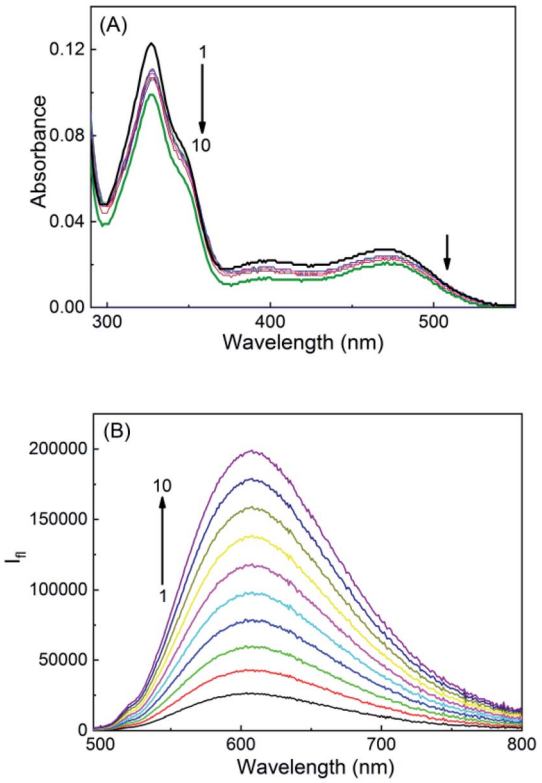

Fig. 8 Absorption (A) and fluorescence (B) spectra of $SBE_7\beta CD:SG^+$ complex at different concentrations of $CaCl_2$ at pH 6.5. $[CaCl_2]$/mM: (1) 0.0, (2) 0.5, (3) 1.5, (4) 4.8, (5) 9.6, (6) 19.0, (7) 32.9, (8) 55.0, (9) 80.3 and (10) 108.2.

demonstrated upward pK_a shift in SGR achieved with the $SBE_7\beta CD$ to increase the antibacterial activity by increasing the equilibrium concentration of SG^+ at pH 7.4 (see Fig. 4). To support this approach, we estimated the effect of $SBE_7\beta CD$ on the antibacterial activity of SGR by examining the growth of four pathogenic micro-organisms, *Bacillus cereus* (*B. cereus*) and *Staphylococcus aureus* (*S. aureus*) (Gram-positive) and *Escherichia coli* (*E. coli*) and *Salmonella typhimurium* (*S. typhimurium*) (Gram-negative) bacteria. Measurements were carried out at pH 7.4 in a 96-well Microtiter plate to evaluate the minimum inhibitory concentration (MIC).[28] After incubating the samples for 18 h, tetrazolium dye was added to each well and further incubated for 20 minutes. The appearance of red colour as shown in Fig. 9 indicates the bacterial growth. The deep red colour suggests intense bacterial growth. The MIC value is evaluated at the concentration when faint red colour or no colour appears. Average MIC values were obtained from all the measurements carried out in duplicate and each repeated thrice (Table S3, ESI†). These values, along with the colour changes in the images provided in Fig. 9 and S6† reveal the reduction in the MIC value of SGR from 14.7 μg ml^{-1} (40 μM) to 7.5 μg ml^{-1} (20 μM) against both *B. cereus* and *E. coli* on complexation with 500 μM $SBE_7\beta CD$ and confirm higher inhibitory effect by the SGR drug in the presence of $SBE_7\beta CD$ in comparison to βCD at the physiological pH (Scheme 2). In case of *S. aureus* (Fig. 9), $SBE_7\beta CD$:SGR complex shows reduction in the MIC value from

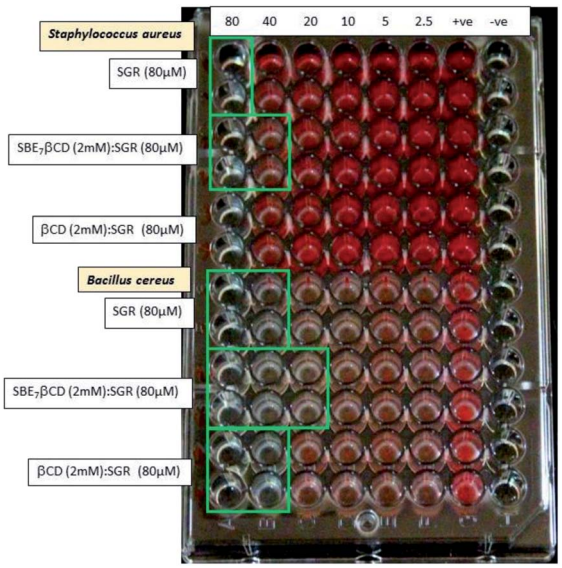

Fig. 9 Antibacterial study of SGR in the absence and presence of $SBE_7\beta CD$ (2 mM) and βCD (2 mM) against *S. aureus* and *B. cereus* at physiological pH 7.4.

29.4 μg ml^{-1} (80 μM) to 14.7 μg ml^{-1} (40 μM) and both SGR and $SBE_7\beta CD$:SGR complex show similar antibacterial activity towards *S. typhimurium* (Fig. S6, ESI†). Alternatively, the antibacterial activity of SGR increased at least by ~two-fold upon complexation with $SBE_7\beta CD$ irrespective of strain of the bacteria used except *S. typhimurium*. This increased activity can be correlated with the upward pK_a shift and enhanced photostability of SGR in the presence of $SBE_7\beta CD$ which results in the increase in the percentage of availability of the active iminium ion. At the same time, control measurements with the addition of only $SBE_7\beta CD$ does not show any effect on the bacterial growth. Moreover, the antibacterial activity of βCD:SGR complex is similar with SGR at pH 7.4 (Fig. 9 and S6†) against these four pathogenic bacteria which indicates that the parent βCD host does not show any effect on the antibacterial activity of SGR. Mechanistically, this is understood as the pK_a value of SGR decreases from 7.5 to 6.55 in the presence of βCD, as a result, the availability of active iminium ion form in the solution at pH 7.4 decreases and hence the antibacterial activity does not display any improvement like the case of SBE_7-βCD:SGR complex.

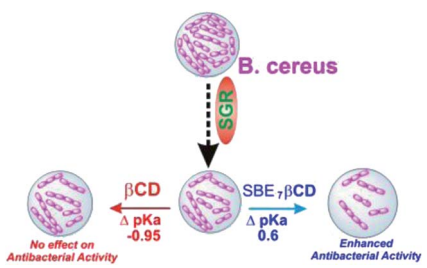

Scheme 2 A schematic representation of the enhanced antibacterial activity of SGR with $SBE_7\beta CD$ and no change in the activity with βCD.

Of late, combination of standard antibiotic drugs with supplements/additives has been quite successful towards multidrug resistant bacteria. In a very recent study we have shown the synergistic effect on the antibacterial activity of ciprofloxacin along with SGR and *p*-sulfonatocalixarene functionalized silver nanoparticles towards multidrug resistant bacteria, *S. oslo*.[14] In the similar line, the ~50% improvement in the antibacterial activity (or 50% reduction in MIC value) documented with the $SBE_7\beta CD$:SGR complex would be promising for combination with standard antibiotic drugs against multi-drug resistant bacteria.

Conclusions

In summary, the host–guest interactions of sulfobutylether-β-cyclodextrin and β-cyclodextrin with the prototropic forms of sanguinarine dye have been investigated by using ground-state optical absorption and steady-state as well as time-resolved fluorescence studies. Photophysical properties of sanguinarine get modulated significantly in the presence of $SBE_7\beta CD$ and has been revealed in the emission intensity features and excited state lifetime parameters. The binding interaction of $SBE_7\beta CD$ with sanguinarine follows the order SG^+ > SGOH, whereas the interaction of parent βCD with sanguinarine follows in the reverse order *i.e.* SGOH > SG^+. Compared with the neutral form of the SGR (SGOH), the protonated form (SG^+) has stronger interactions with the $SBE_7\beta CD$ host, leading to considerable changes in the protolytic equilibrium of the dye. $SBE_7\beta CD$ causes upward shift in pK_a value of sanguinarine by more than 0.6 units and makes the guest more basic, because $SBE_7\beta CD$ stabilizes the protonated form of the dye by cation–anion interactions than the neutral form, SGOH. The upward shift in the pK_a value has been utilized to increase the availability of the biologically active iminium form of SGR for the antibacterial activity at physiological pH. An enhanced antibacterial efficacy, and reduced MIC value of SGR against three pathogenic bacteria, *i.e. E. coli*, *S. aureus* and *B. cereus* have been achieved by introducing $SBE_7\beta CD$ host in to the system. On the other hand, the spectroscopic features, especially the emission was shown to be modulated in the presence of external stimuli such as metal ions. Upon the addition of Ca^{2+} ion, nearly quantitative dissociation of the complex was established to regenerate the fluorescence of free dye. Such supramolecular pK_a shifts in the prototropic guest upon formation of inclusion complexes with macrocyclic hosts and their stimuli-responsive behavior are of great current research interest, because they find potential applications in drug delivery, catalysis, sensor and as improved antibacterial, anticancer agents.

Conflicts of interest

There are no conflicts to declare.

Acknowledgements

We gratefully acknowledge the support and encouragement from the host institute, Bhabha Atomic Research Centre, for this research work. We acknowledge the support from Dr Awadhesh Kumar, Head, RPCD, Dr A. K. Tyagi, Associate Director, Chemistry Group and Dr S. K. Ghosh, Associate Director, Bio Science Group, BARC, Mumbai.

References

1 (*a*) R. Khurana, N. Barooah, A. C. Bhasikuttan and J. Mohanty, *ChemPhysChem*, 2019, **20**, 2498; (*b*) M. N. Shinde, A. C. Bhasikuttana and J. Mohanty, *Supramol. Chem.*, 2016, **28**, 517.
2 R. Khurana, S. Agarwalla, G. Sridhar, N. Barooah, A. C. Bhasikuttan and J. Mohanty, *ChemPhysChem*, 2018, **19**, 2349.
3 R. Khurana, J. Mohanty, N. Padma, N. Barooah and A. C. Bhasikuttan, *Chem.–Eur. J.*, 2019, **25**, 13939.
4 M. Sayed, F. Biedermann, V. D. Uzunova, K. I. Assaf, A. C. Bhasikuttan, H. Pal, W. M. Nau and J. Mohanty, *Chem.–Eur. J.*, 2015, **21**, 691.
5 (*a*) R. Khurana, N. Barooah, A. C. Bhasikuttan and J. Mohanty, *Org. Biomol. Chem.*, 2017, **15**, 8448; (*b*) N. Barooah, A. Kunwar, R. Khurana, A. C. Bhasikuttan and J. Mohanty, *Chem.–Asian J.*, 2017, **12**, 122.
6 H. S. El-Sheshtawy, S. Chatterjee, K. I. Assaf, M. N. Shinde, W. M. Nau and J. Mohanty, *Sci. Rep.*, 2018, **8**, 13925.
7 G. Ping, Y. Wang, L. Shen, Y. Wang, X. Hu, J. Chen, B. Hu, L. Cui, Q. Meng and C. Li, *Chem. Commun.*, 2017, **53**, 7381.
8 N. Singh and B. Sharma, *Front. Mol. Biosci.*, 2018, **5**, 21.
9 J.-Y. Xu, Q.-H. Meng, Y. Chong, Y. Jiao, L. Zhao, E. M. Rosen and S. Fan, *Oncol. Rep.*, 2012, **28**, 2264.
10 S. Hazra and G. S. Kumar, *RSC Adv.*, 2015, **5**, 1873.
11 M. Maiti, R. Nandi and K. Chaudhuri, *Photochem. Photobiol.*, 1983, **38**, 245.
12 F. Miao, X.-J. Yang, L. Zhou, H.-J. Hu, F. Zheng, X.-D. Ding, D.-M. Sun, C.-D. Zhou and W. Sun, *Nat. Prod. Res.*, 2011, **25**, 863.
13 R. Hamoud, J. Reichling and M. Wink, *J. Pharm. Pharmacol.*, 2015, **67**, 264; R. Hamoud, J. Reichling and M. Wink, *Drug Metab. Lett.*, 2014, **8**, 119.
14 C. Mehra, R. Gala, A. Kakatkar, V. Kumar, R. Khurana, S. Chatterjee, N. N. Kumar, N. Barooah, A. C. Bhasikuttan and J. Mohanty, *Chem. Commun.*, 2019, **55**, 14275.
15 Z. Miskolczy, M. Megyesi, G. Tarkanyi, R. Mizsei and L. Biczok, *Org. Biomol. Chem.*, 2011, **9**, 1061.
16 (*a*) T. Loftsson and M. E. Brewster, *J. Pharm. Sci.*, 1996, **85**, 1017; (*b*) N. Sharma and A. Baldi, *Drug Delivery*, 2016, **23**, 729–747.
17 M. N. Shinde, A. C. Bhasikuttan and J. Mohanty, *ChemPhysChem*, 2015, **16**, 3425.
18 M. N. Shinde, R. Khurana, N. Barooah, A. C. Bhasikuttan and J. Mohanty, *J. Phys. Chem. C*, 2017, **121**, 20057.
19 R. Khurana, A. S. Kakatkar, S. Chatterjee, N. Barooah, A. Kunwar, A. C. Bhasikuttan and J. Mohanty, *Front. Chem.*, 2019, **7**, 452.
20 J. R. Lakowicz, '*Principles of Fluorescence Spectroscopy*', Springer, 2006.

21 J. Li, B. Li, Y. Wu, S. Shuang, C. Dong and M. M. F. Choi, *Spectrochim. Acta*, 2012, **95**, 80.
22 M. K. Singh, H. Pal, A. S. R. Koti and A. V. Sapre, *J. Phys. Chem. A*, 2004, **108**, 1465.
23 (*a*) J. Mohanty, A. C. Bhasikuttan, W. M. Nau and H. Pal, *J. Phys. Chem. B*, 2006, **110**, 5132; (*b*) M. Shaikh, J. Mohanty, P. K. Singh, W. M. Nau and H. Pal, *Photochem. Photobiol. Sci.*, 2008, **7**, 408.
24 I. Ghosh and W. M. Nau, *Adv. Drug Delivery Rev.*, 2012, **64**, 764.
25 (*a*) N. Saleh, A. L. Koner and W. M. Nau, *Angew. Chem., Int. Ed.*, 2008, **47**, 5398; (*b*) M. Shaikh, J. Mohanty, A. C. Bhasikuttan, V. D. Uzunova, W. M. Nau and H. Pal, *Chem. Commun.*, 2008, 3681; (*c*) M. Shaikh, S. Dutta Choudhury, J. Mohanty, A. C. Bhasikuttan, W. M. Nau and H. Pal, *Chem.–Eur. J.*, 2009, **15**, 12362; (*d*) K. Vasu, R. Khurana, J. Mohanty and S. Kanvah, *RSC Adv.*, 2018, **8**, 16738; (*e*) R. Wang, L. Yuan and D. H. Macartney, *Chem. Commun.*, 2005, 5867; (*f*) V. S. Kalyani, D. D. Malkhede and J. Mohanty, *Phys. Chem. Chem. Phys.*, 2017, **19**, 21382.
26 M. J. Frisch, G. W. Trucks, M. Head-Gorden, P. M. W. Gill, M. W. Wong, J. B. Foresman, B. G. Johnson, H. B. Schlegel, M. A. Robb, E. S. Replogle, R. Gomperts, J. L. Andres, K. Rahavachari, J. S. Binkley, C. Gonzalez, R. Martin, L. D. J. Fox, D. J. Defrees, J. Baker, J. J. P. Stewart and J. A. Pople, *Gaussian 92*, Gaussian Inc., Pittsburgh, PA, 1992.
27 (*a*) J. Mohanty and W. M. Nau, *Angew. Chem., Int. Ed.*, 2005, **44**, 3750; (*b*) W. M. Nau and J. Mohanty, *Int. J. Photoenergy*, 2005, **7**, 133; (*c*) J. Mohanty, H. Pal, A. K. Ray, S. Kumar and W. M. Nau, *ChemPhysChem*, 2007, **8**, 54; (*d*) J. Mohanty, K. Jagtap, A. K. Ray, W. M. Nau and H. Pal, *ChemPhysChem*, 2010, **11**, 3333; (*e*) A. C. Bhasikuttan, H. Pal and J. Mohanty, *Chem. Commun.*, 2011, **47**, 9959.
28 Clinical and Laboratory Standards Institute (CLSI), in *Performance Standards for Antimicrobial Susceptibility Testing; Twenty-Third Informational Supplement, M100-S23*, Wayne, PA, USA, 2013, vol. 34:1.

